Decomposed Phase Analysis using Convex Inner Approximations: a Methodology for DER Hosting Capacity in Distribution Systems

Hani Mavalizadeh, Mads R. Almassalkhi

Department of Electrical and Biomedical Engineering

University of Vermont

Burlington, USA

{hmavaliz, malmassa}@uvm.edu

Abstract—This paper uses convex inner approximations (CIA) of the AC power flow to tackle the optimization problem of quantifying a three-phase distribution feeder's capacity to host distributed energy resources (DERs). This is often connoted hosting capacity (HC), but herein we consider separative bounds for each node on positive and negative DER injections, which ensures that injections within these nodal limits satisfy feeder voltage and current limits and across nodes sum up to the feeder HC. The methodology decomposes a three-phase feeder into separate phases and applies CIA-based techniques to each phase. An analysis is developed to determine the technical condition under which this per-phase approach can still guarantee three-phase constraints. New approaches are then presented that modify the per-phase optimization problems to overcome conservativeness inherent to CIA methods and increase HC, including selectively modifying the per-phase impedances and iteratively relaxing per-phase voltage bounds iterative method has been proposed to modify the voltage bounds. Discussion is included on trade-offs and feasibility. To validate the methodology simulation-based analysis is conducted with the IEEE 37-node test feeder and a real 534-node unbalanced radial distribution feeder.

Index Terms—Distributed energy resources, convex optimization, hosting capacity, distribution system, three-phase power.

I. INTRODUCTION

As the deployment of distributed energy resources (DERs) in power grids continues to accelerate, their utilization in a number of ancillary services is increasing [1]. In this context, DERs can be managed by aggregators, which dispatch them in response to market signals, often without taking into account the limitations of the grid. This lack of consideration can potentially lead to violations of critical grid constraints, including voltage and transformer limits. Therefore, there is an urgent need for what is referred to as *Grid-aware DER coordination*, which involves effectively accounting for AC network constraints during the coordination of DERs [2].

Various methods have been proposed in the technical literature for grid-aware DER coordination. One common approach is to restrict the amount of power that each customer can export to the grid [3]. However, this method can be overly conservative, and with the rapid increase in the number of DERs connected to the grid, these fixed limits can become outdated and require frequent updates [4].

In direct control schemes, it is assumed that the grid operator has access to all DER data and can directly control DERs [5], [6]. While direct control methods can theoretically provide optimal solutions, they often rely on strong assumptions related to observability and controllability. In practice, DER aggregators do not have access to grid data, and grid operators do not have full control over DERs.

Alternatively, [7] proposes an approach where the grid operator adjusts locational marginal prices (LMPs) based on grid conditions to incentivize the aggregator to adapt the DER aggregate load accordingly. However, this paper assumes a balanced distribution system, which may not hold in real-world applications. In [8], two mechanisms are presented to allow the grid operator to override DER aggregator dispatch decisions to ensure grid constraints are not violated. One limitation is that in certain electric markets, the grid operator may not have the authority to block aggregator control decisions.

Another approach is for the grid operator to establish limits on the amount of injection from each node to preserve grid constraints. This approach requires minimal information exchange between the grid operator and aggregator. In [4], the concept of *operating envelopes* is introduced, where the grid operator uses linear or model-free methods to issue time-varying export/import limits to aggregators. A convex inner approximation (CIA) is presented in [9] for maximizing voltage margins, which is generalized in [10] to compute feeder hosting capacity of balanced or single-phase distribution feeders. In [11], a sequential algorithm is presented that constructs a convex restriction around an initial feasible point, subsequently refining it to obtain an improved feasible solution. This work is extended further in [12], where the approach is enhanced to account for robustness against uncertainty in power injections. In [13], a model-free approach is introduced, leveraging historical meter data and neural networks to eliminate the need for solving the non-convex AC OPF problem in unbalanced distribution feeders. It demands access to substantial volumes

of meter data, which may not always be readily available. Additionally, it's important to note that model-free methods can exhibit sensitivity to the quality and distribution of data. In [14] a bottom-up approach is presented where DERs submit power injection requests based on their local controllers to the grid operator. The grid operator can deny injection requests if a three-phase power flow analysis indicates a risk of grid constraint violation. An optimization model for assessing the hosting capacity (HC) of DERs, taking into consideration the anticipated network conditions during demand response scheduling and adapting to the real-time network state is developed in [15].

Thus, in the literature there are either simplified models used to compute hosting capacities with no guarantees or guarantees applicable only for simplified systems. It is within this context that this paper contributes to the field of computing hosting capacity for realistic systems with outlined trade-offs between optimality and guaranteed feasibility:

- The recently presented optimization-based approach for computing hosting capacity of single-phase distribution feeders in [10] has been extended to three-phase, unbalanced distribution feeders. An analysis is also conducted to provide technical conditions under which our proposed per-phase HC estimates can be combined to guarantee that 3-phase phase grid constraints are satisfied.
- The HC estimate for unbalanced feeders is then improved by iteratively adjusting voltage bounds within the per-phase optimization framework, accounting for mutual impedances and unbalanced loadd in the 3-phase system.
- Finally, the methodology is validated through simulation-based analysis on the IEEE 37-node feeder and a real 3-phase network with more then 500 three-phase nodes.

The remainder of the paper is organized as follows: Section II provides a concise overview of the preliminary concepts used in this paper. The proposed approach to extend the CIA-based method to three-phase unbalanced grids is presented in Section III. In Section IV, an approach for ensuring grid constraint satisfaction is detailed. Section V introduces an iterative method designed to enhance HC. Finally, numerical results are provided in Section VI followed by concluding remarks in Section VII.

II. PRELIMINARIES

This section describes the modeling of distribution feeders and their hosting capacity (HC). The CIA-based approach detailed in [9], [10] employs a CIA of the set of feasible admissible injections. An optimization problem is used to determine the HC at each node of a distribution feeder. The total feeder HC is the sum across all nodes. We aim to adapt this for unbalanced feeders. Next, we discuss the single-phase equivalent load flow, i.e., *DistFlow* [16], and the convex HC formulation.

A. Balanced feeder HC via convex inner approximations

Consider a radial (single-phase) distribution feeder as a tree graph $G = (\mathcal{V}, \mathcal{E})$ with N nodes $\mathcal{V} := \{1, \ldots, N\}$ and $N - 1$

branches $\mathcal{E} \subseteq \mathcal{V} \times \mathcal{V}$, such that if nodes i and j are connected, then $(i, j) \in \mathcal{E}$. At each node $i \in \mathcal{V}$, *DistFlow* considers the square of the voltage phasor magnitude, i.e., $V_i := |v_i|^2$ and complex power injections are denoted $s_i = p_i + \mathbf{j}q_i$. Node 0 is assumed to be the substation (slack) node with a fixed voltage V_0. Through each branch with impedance $z_{ij} = r_{ij} + \mathbf{j}x_{ij}$, we consider the square of the current phasor, i.e., $l_{ij} := |I_{ij}|^2$ and the active and reactive power flows, P_{ij} and Q_{ij}. Thus, from the *DistFlow* formulation and applying [17], the relationships between voltages and branch power flows and nodal injections and line currents can be defined as

$$V = V_0 \mathbf{1}_N + M_p p + M_q q - Hl \tag{1a}$$

$$P = Cp - D_R l \tag{1b}$$

$$Q = Cq - D_X l, \tag{1c}$$

where appropriately-sized matrices M_p, M_q, H, C, D_R, D_X are detailed in [9], [10] and serve to map injections and currents to corresponding voltages and branch power flows across the network. Besides the linear equations in (1), the *DistFlow* also relates voltages and power flows to currents via non-convex

$$l_{ij}(P, Q, V) = (P_{ij}^2 + Q_{ij}^2)/V_i. \tag{2}$$

The non-linear (2) makes the *DistFlow* formulation non-convex within an optimal power flow (OPF) setting. Thus, we are interested in utilizing a CIA of the *DistFlow* formulation. The CIA effectively bounds the nonlinear l_{ij} with a convex envelope: $l^-(P, Q, V) \leq l_{ij}(P, Q, V) \leq l^+(P, Q, V)$, which enables the creation of two sets of variables: upper ($^+$) and lower proxies ($^-$), e.g., $V^- \leq V \leq V^+$. As long as the lower proxies satisfy lower limits and upper proxies satisfy upper limits, e.g., $\underline{V} \leq V^-$ and $V^+ \leq \bar{V}$, then we are guaranteed that the physical variable satisfies, e.g., $\underline{V} \leq V \leq \bar{V}$. This guarantee means that we can replace the physical variables altogether and replace them with their convex proxies.

Consider for example a feeder with inductive branches, i.e., $x_{ij} > 0$, $\forall (i, j) \in \mathcal{E}$ [9]. Then, we can replace the non-convex formulation in (1) and (2) with their convex proxies:

$$V^+ = V_0 \mathbf{1}_N + M_p p + M_q q - Hl^- \tag{3a}$$

$$V^- = V_0 \mathbf{1}_N + M_p p + M_q q - Hl^+ \tag{3b}$$

$$P^+ = Cp - D_R l^- \tag{3c}$$

$$P^- = Cp - D_R l^+ \tag{3d}$$

$$Q^+ = Cq - D_X l^- \tag{3e}$$

$$Q^- = Cq - D_X l^+. \tag{3f}$$

$$l^+ \geq f_{\text{quad}}(P^+, P^-, Q^+, Q^-, V^+, V^-) \tag{3g}$$

$$l^- := f_{\text{aff}}(P^+, P^-, Q^+, Q^-, V^+, V^-), \tag{3h}$$

where l^- is affine in the proxy variables while l^+ is a convex relaxation of a quadratic function of the proxy variables. Please see Appendix A for derivations of f_{aff} and f_{quad} and [9], [10] for full details. Finally, the feeder HC is then the maximum sum of nodal injections, $p_i^+ := p_i^*$, that drives the feeder to its capacity (e.g., voltage, current, or power flow limits are

active). The convex formulation that achieves this objective is

$$\mathbf{P}_{\text{CIA}}^{\phi,+}: \quad p^+ := \arg\max_{p_i} \sum_{i=1}^{N} w_i p_i \tag{4a}$$

$$\text{subject to (3)} \tag{4b}$$

$$\underline{l} \le l^- \qquad l^+ \le \bar{l} \tag{4c}$$

$$\underline{V} \le V^- \quad V^+ \le \overline{V} \tag{4d}$$

$$p_i^2 + q_i^2 \le \overline{s_i}^2, \quad \forall i \in \mathcal{V}, \tag{4e}$$

where w_i are design parameters that differentiate nodal capacities. Note that inequality (4e) is optional and captures limits on active injections based on apparent power limits at each node (e.g., from inverter, transformer, or power factor limits). Other constraints on $P^{+/-}, Q^{+/-}$ may also be added.

The HC for DER injections (e.g., solar PV) is defined as

$$\overline{\text{HC}} := \sum_{i}^{N} p_i^+ = \mathbf{1}_N^\top p^+ > 0. \tag{5}$$

Similarly, we can define the HC relative to consumption (e.g., electric vehicle HC) as $\underline{\text{HC}} := \sum_{i}^{N} p_i^- = \mathbf{1}_N^\top p^- < 0$, where p^- is the solution that minimizes the nodal (net) injections, i.e.,, solve corresponding $\mathbf{P}_{\text{CIA}}^{\phi,-}$ problem, whose details are omitted due to page limits. Thus, $\underline{\text{HC}} \le 0 \le \overline{\text{HC}}$.

However, since $\mathbf{P}_{\text{CIA}}^{\phi,+}$ and $\mathbf{P}_{\text{CIA}}^{\phi,-}$ employ a CIA of *Dist-Flow*, the HC estimates are valid only for balanced, radial distribution feeders. We are now interested in how to adapt this CIA-based method to a realistic unbalanced distribution feeder, which means that we need to consider the effects of mutual phase impedance and load unbalances.

B. Unbalanced distribution power flow

Consider a three-phase, radial graph G, wherein each node represents three phases: a, b, c. Similarly, each branch represents a three-phase line section with a corresponding 3×3 impedance matrix, which is expressed as,

$$z_{ij}^{3\phi} := \begin{bmatrix} z_{ij}^{\text{a}} & z_{ij}^{\text{ab}} & z_{ij}^{\text{ac}} \\ z_{ij}^{\text{ba}} & z_{ij}^{\text{b}} & z_{ij}^{\text{bc}} \\ z_{ij}^{\text{ca}} & z_{ij}^{\text{cb}} & z_{ij}^{\text{c}} \end{bmatrix} \forall (i,j) \in \mathcal{E}. \tag{6}$$

Voltage at 3-phase node i is denoted $V_i^{3\phi} = \begin{bmatrix} V_i^a, V_i^b, V_i^c \end{bmatrix}^\top$ and current in branch $(i,j) \in \mathcal{E}$ is $I_{ij}^{3\phi} = \begin{bmatrix} I_{ij}^a, I_{ij}^b, I_{ij}^c \end{bmatrix}^\top$. The line voltage drop and currents are related by

$$\Delta V_{ij}^{3\phi} := V_i^{3\phi} - V_j^{3\phi} = z_{ij}^{3\phi} I_{ij}^{3\phi} \Rightarrow \Delta V^{3\phi} = Z^{3\phi} I^{3\phi}, \tag{7}$$

where, $I^{3\phi} = [I_{ij}^{3\phi}]_{(i,j)\in\mathcal{E}} \in \mathbb{C}^{3(N-1)}$ represents the complex three-phase currents, $V^{3\phi} = [V_i^{3\phi}]_{i\in\mathcal{V}} \in \mathbb{C}^{3N}$ corresponds to the three-phase voltages, $Z^{3\phi} \in \mathbb{C}^{3(N-1)\times 3(N-1)}$ is the complex three-phase impedance matrix

Next, we seek to extend the CIA-based method from balanced (single-phase equivalent) feeders to unbalanced feeders.

III. EXTENDING CIA TO UNBALANCED FEEDERS

Given an unbalanced feeder, how can we approximate or decompose it for HC analysis? In this section, we seek to answer this question. Specifically, we consider methods for 1) approximating feeders as balanced (e.g., by modifying line impedances and nodal loads and 2) decomposing feeders along their phases. These are summarized next.

- **Method 1 - balanced feeder approximation:** This strategy involves transforming an unbalanced feeder into an *approximate* balanced model, which is then used to determine p^-, p^+ from $\mathbf{P}_{\text{CIA}}^{\phi,+\backslash-}$. The resulting per-phase HC is then distributed equally to each phase. We consider two different ways to approximate a balanced feeder:
  i) Take the maximum line impedance and minimum loads across all three phases to capture the worst-case voltage drop/rise.
  ii) Average line impedances and loads across phases a/b/c to create a balanced approximation of a feeder. This approximation can potentially cause voltage violations at the corresponding HC value.
- **Method 2 - per-phase analysis:** In this approach, we extract each phase separately and compute p^- and p^+. This per-phase approach is considered for two different implementations:
  i) One phase is selected and nodal HC values, (p_i^-, p_i^+), are computed for that phase. For the 3-phase feeder, the same (p_i^-, p_i^+) values are then applied to all phases at a three-phase node. We denote the sub-methods $2i^\phi$ for $\phi = \{a, b, c\}$, e.g., $\overline{\text{HC}}_{3\phi} = 3 \times \mathbf{1}_N^\top p_a^+$ for method $2i^a$.
  ii) All three phases are extracted separately and we compute (p^-, p^+) for each phase, which yields hosting capacity, e.g., $\overline{\text{HC}}_{3\phi} = \mathbf{1}_N^\top (p_a^+ + p_b^+ + p_c^+)$.

Each of these methods estimate the three-phase HC, e.g., $\overline{\text{HC}}$ by computing net nodal injections, e.g., p_ϕ^+, which are then applied to the full three-phase network to determine the corresponding three-phase voltages and currents. In Fig.1, these voltage and current profiles for Method 2ii are presented for the IEEE 37-node test feeder [18]. As can be seen, despite single-phase analysis underpinning the HC estimate, phase voltages are within $\overline{V} = 1.05$ pu across all nodes and phases. Next, we are interested in metrics that can be used to compare the different methods.

- **Total number of violations**, N_v, counts the number of nodes and phases for which $|V_i^{3\phi}| \notin [\underline{V}, \overline{V}]$.
- **Maximum violation in per unit**, M_v, provides a measure of the severity of the violations:

$$M_v = \max_{i=1,\dots,3N} \left\{ \max \left\{ 0, E_i^{\text{u}}, E_i^{\text{l}} \right\} \right\}, \tag{8}$$

where, $E^{\text{u}} := |V^{3\phi}| - \overline{V} \mathbf{1}_{3N}$ and $E^{\text{l}} := \underline{V} \mathbf{1}_{3N} - |V^{3\phi}|$.
- **Sum of violations**, S_v, captures the cumulative severity of violations across the network:

$$S_v = \sum_{i=1}^{3N} \max \left(0, E_i^{\text{u}}, E_i^{\text{l}} \right). \tag{9}$$
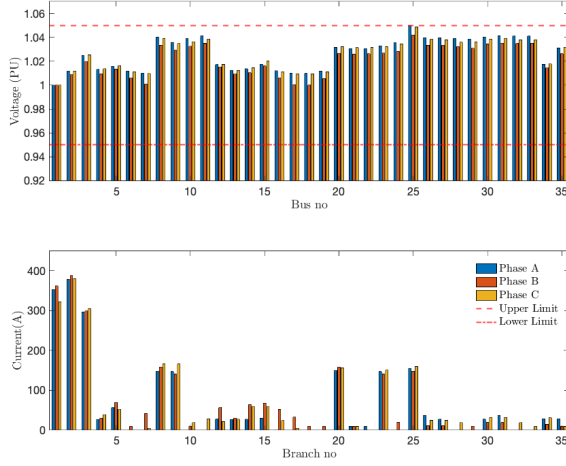
Fig. 1. Illustrating the effects of Method 2ii on three-phase voltage and current profiles following the addition of nodal injections $p_a^+ + p_b^+ + p_c^+$. The dashed red line indicates the ANSI voltage limits of [0.95, 1.05] pu.

- **Average voltage margin**, W_M, measures how conservative the HC results from $\mathbf{P}_{\text{CIA}}^{\phi,+/-}$ are:

$$W_M = \frac{1}{3N} \sum_{i=1}^{3N} \max\{0, \Delta W_i\}, \qquad (10)$$

where $\Delta W_i := \min\left\{|V_i^{3\phi}| - \underline{V}, \overline{V} - |V_i^{3\phi}|\right\}$.

- **Voltage unbalance factor (VUF)** provides a relative measure (in %) of voltage unbalance caused by nodal HC injections:

$$\text{VUF} = \frac{100}{N} \sum_{i=1}^{N} \frac{\max\left\{|V_i^{3\phi}| - \frac{1}{3}\mathbf{1}_3^\top |V_i^{3\phi}|\mathbf{1}_3\right\}}{\frac{1}{3}\mathbf{1}_3^\top |V_i^{3\phi}|}. \qquad (11)$$

Table I uses the metrics above to compare HC estimates, i.e., using $\mathbf{P}_{\text{CIA}}^{\phi,+}$. Notably, the comparison shows that Method 2ii provides the largest HC without incurring any voltage violations. It should be noted that although the HC is larger in method 2i^c, the corresponding nodal HC injections cause undesirable voltage violations.

Given that Method 2ii uses information from all phases without averaging, it is somewhat expected that Method 2ii could outperform the other approaches. Of course, when optimizing nodal injections across phases separately can lead to (net) load imbalances that cause larger VUF (but still well within typical 2% limits). Nonetheless, results in Table I justifies the selection of Method 2ii for further analysis.

It is important to note that HC results obtained from per-phase analysis with $\mathbf{P}_{\text{CIA}}^{\phi,+}$ and $\mathbf{P}_{\text{CIA}}^{\phi,-}$ can result in voltage violations when applied to unbalanced networks, including for Method 2ii This is because per-phase methods neglect mutual impedances. In the next section, technical conditions are presented under which per-phase analysis and HC optimization extend to three-phase networks.

TABLE I
PERFORMANCE OF THE PROPOSED METHODS

Method	N_v	M_v(pu)	VUF (%)	S_v (pu)	W_M (pu)	$\overline{\text{HC}}$ (MW)
1i	0	0	0.21	0	0.026	15.33
1ii	1	0.001	0.23	0.001	0.025	15.55
2i^a	0	0	0.22	0	0.025	15.20
2i^b	0	0	0.22	0	0.029	15.54
2i^c	3	0.003	0.23	0.005	0.023	15.94
2ii	0	0	0.33	0	0.025	15.57

IV. GUARANTEEING THREE-PHASE GRID CONSTRAINTS

In this section, we present an approach for adapting the per-phase HC estimates while guaranteeing no voltage violations when applied to the full three-phase network. The method effectively modifies the impedance matrix. We also modify the approach to adjust the conservativeness and show that the corresponding voltage violations are significantly reduced. The approach makes the following assumptions:

Assumption 1. *The sum of the phase load currents is zero.*

Assumption 2. *Three-phase lines are transposed, such that mutual impedances are identical:* $z_{ij}^{3\phi} = \begin{bmatrix} z_{ij}^a & z_{ij}^m & z_{ij}^m \\ z_{ij}^m & z_{ij}^b & z_{ij}^m \\ z_{ij}^m & z_{ij}^m & z_{ij}^c \end{bmatrix}.$

From the above assumptions, the following theorem holds.

Theorem 1. *Given a 3-phase system that satisfies Assumptions 1 and 2, if per-phase optimization $\mathbf{P}_{CIA}^{\phi,+}$ satisfies $\underline{V} \leq V_i(p^+) \leq \overline{V} \ \forall i \in \mathcal{V}$, then the three-phase system satisfies $\underline{V} \leq V_i^{3\phi}(p^+) \leq \overline{V} \ \forall i \in \mathcal{V}$. Same holds for $\mathbf{P}_{CIA}^{\phi,-}$ and $V_i(p^-)$.*
Proof: *please see Appendix B.*

Theorem 1 states when a three-phase distribution feeder can be decomposed into three decoupled single-phase distribution systems with modified impedances, $z_{ij}^\phi - z_{ij}^m$, to provide guarantees that the resulting HC will not engender voltage violations in the three-phase system.

Remark 1. *Using a similar approach, and by further assuming identical conductor impedances $z_{ij}^a = z_{ij}^b = z_{ij}^c$, Theorem 1 extends to Delta-connected loads.*

To illustrate Theorem 1, we briefly modify the IEEE 37-node feeder by setting all mutual impedances equal to z_{ij}^{ab}, while simultaneously matching the loadings of phases b and c to that of phase a.

From each phase, we construct a sub-feeder from which we can compute nodal HC (net) injections p_i^- and p_i^+ using Method 2ii. The resulting voltages of the single-phase networks, $|V_i|$, are then compared with those of the full 3-phase load flow, $|V_i^{3\phi}|$, with the 3-phase (net) injections $p_{3\phi}^+ := [p_{a,i}^+, p_{b,i}^+, p_{c,i}^+]_{i \in \mathcal{V}}$ added to the system load.

In Fig. 2, a scatter plot of three-phase and single-phase voltage magnitudes is provided, i.e., $|V_i^{3\phi}|$ vs. $|V_i|$ for the modified IEEE 37-node system. The red dots represent $|V_i^{3\phi}|$
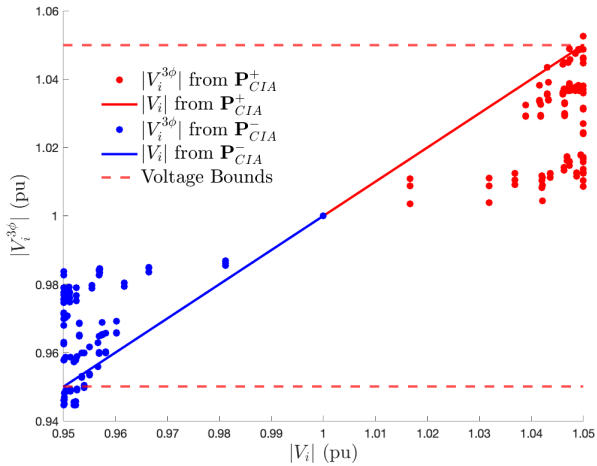
Fig. 2. Comparison between three-phase and single-phase voltages for the modified IEEE 37-node system. The dashed red lines indicate the voltage limits.
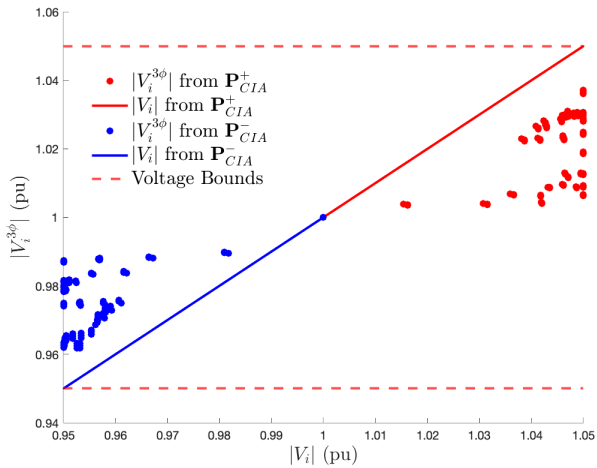

Fig. 3. Three-phase voltages after modifying the impedance matrix based on Theorem 1 for the IEEE 37-node system.

with injections $p_{3\phi}^+$ added and the blue dots correspond to $|V_i^{3\phi}|$ when $p_{3\phi}^-$ is added. As expected, voltage violations arise from unmodeled unbalanced loads and mutual impedances.

To mitigate the voltage violations, we adjust the impedance matrix per Theorem 1. Specifically, in $\mathbf{P}_{CIA}^+$ and $\mathbf{P}_{CIA}^-$, the impedance of each line is augmented by mutual impedance (z_{ij}^m), which is set to be the same for all phases (z_{ij}^m) in the modified test system. It should be noted that using the modified impedance in $\mathbf{P}_{CIA}^+$ and $\mathbf{P}_{CIA}^-$ successfully eliminates voltage violations. However, it comes at the cost of a significantly reduced HC. Specifically, $\overline{HC}$ decreases from 15.6 MW to 12.3 MW (a 20% reduction), while $\underline{HC}$ decreases from 9.0 to 6.0 MW (a 33 % reduction). The large drop in estimated HC is, in large part, due to the margins added at every node in each phase. We denote the approach to solving $\mathbf{P}_{CIA}^-$ with modified impedance from Theorem 1 as **Mod-Z** HC.

TABLE II
THE IMPACT OF MODIFYING THE IMPEDANCE MATRIX ON HC AND VOLTAGE VIOLATIONS FOR THE MODIFIED IEEE 37-NODE SYSTEM.

ϵ (pu)	0	0.0005	0.0010	Method 2ii
$\overline{HC}$ (MW)	12.31	15.47	15.47	15.55
$\underline{HC}$ (MW)	-6.02	-8.88	-8.89	-8.96
# violations	0	0	2	6
# modified lines	36	5	2	-

In the remainder of this section, we present a simulation-based approach to adjust the impedance matrix in Mod-Z to reduce the voltage violations. Thus, instead of (naively) altering the impedance for all branches at once, the branches connected to nodes with simulated voltage violations are not modified. Specifically, we modify the impedance of lines connected to nodes which satisfy the following condition,

$$|V_i^{3\phi}| - |V_i| < \epsilon \quad \forall i, \tag{12}$$

where ϵ is a design parameter that allows us to limit the number of line modifications. The more lines we modify, the larger HC we get, but with the downside of more voltage violations. No free lunch in engineering.

To explore this tradeoff further, Table II tabulates the effects of different ϵ values in the Mod-Z approach. Clearly, with $\epsilon = 0.001$ pu, only 5 of 36 lines are modified, all voltage violations are eliminated, and the increase in HC is more than 26%. That is pretty close to a free lunch. We denote the approach of solving $\mathbf{P}_{CIA}^{+/-}$ with modified impedance from Theorem 1 as **Mod-Z** HC.

This section showed the value of selectively modifying line impedances to enable per-phase optimization to apply directly to unbalanced distribution systems. Next, we seek to further enlarge the three-phase HC by not just modifying impedances of each phase, but also by (incrementally) relaxing voltage bounds in the per-phase optimization formulation.

V. ITERATIVE VOLTAGE BOUNDS TO INCREASE HC

In this section, a novel approach is introduced that incrementally improves the three-phase HC estimate by coupling 3-phase load flows with per-phase optimization $\mathbf{P}_{CIA}^{\phi,+\backslash-}$. The proposed Method is summarized in Fig. 4 and outlined as follows for p^+ $\overline{HC}$ (the approach is similar for p^- and $\underline{HC}$):

Step 1: *Single-phase optimization*: given per-phase voltage bounds $\underline{V}$ and $\overline{V}$, solve $\mathbf{P}_{CIA}^+$ for each phase using Method 2ii to get nodal HC values p_ϕ^+ and $\overline{HC}_\phi$.

Step 2: *Single-phase load flow*: Apply p_ϕ^+ to each phase ϕ and perform single-phase load flow: V_ϕ^{per} and I_ϕ^{per}.

Step 3: *Three-phase load flow*: Apply $\{p_\phi^-\}_{\phi=\{a,b,c\}}$ to 3-phase system and perform load flow: $V^{3\phi}$ and $I^{3\phi}$.

Step 4: *Termination condition*: The algorithm stops if any element of $|V_i^{3\phi}|$ exceeds $[\underline{V}, \overline{V}]$.

Step 5: *Estimate per-phase voltage*: The per-phase model ignores mutual impedances, which leads to a voltage difference across phases relative to the three-phase model. To estimate this difference, consider (7) and
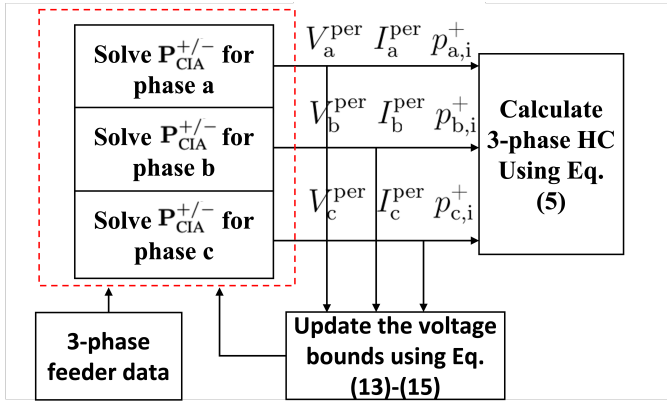
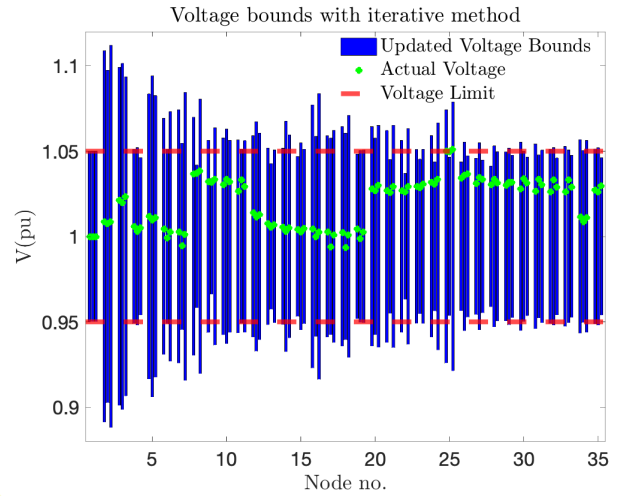Fig. 4. Flowchart of the proposed iterative voltage bound approach.

Fig. 5. Voltage bounds upon termination of the iterative method for $\mathbf{P}_{\text{CIA}}^{\phi,+}$.

TABLE III
COMPARING THE DIFFERENT METHODS ACROSS TWO NETWORKS.

Network	Method 2ii		Iterative HC		Mod-Z	
	$\underline{\text{HC}}$	$\overline{\text{HC}}$	$\underline{\text{HC}}$	$\overline{\text{HC}}$	$\underline{\text{HC}}$	$\overline{\text{HC}}$
IEEE 37						
HC (MW)	-9.0	15.6	-9.5	17.0	-9.2	19.6
Run Time (s)	50	58	133	124	49	61
Real Feeder						
HC (MW)	-42.3	70.7	-71.2	79.2	-24.8	46.6
Run time (s)	148	209	613	422	221	237

assume currents $I_{ij}^{\phi} \approx I_{ij,\phi}^{3\phi}$ are common across both the per-phase and three-phase systems. Then, the estimated voltage for each phase becomes,

$$V_j^{\text{est}} = V_i^{\text{est}} - \begin{bmatrix} z_{ij}^{\text{a}} & z_{ij}^{\text{ab}} & z_{ij}^{\text{ac}} \\ z_{ij}^{\text{ba}} & z_{ij}^{\text{b}} & z_{ij}^{\text{bc}} \\ z_{ij}^{\text{ca}} & z_{ij}^{\text{cb}} & z_{ij}^{\text{c}} \end{bmatrix} I_{ij}^{3\phi} \quad \forall (i,j) \in \mathcal{E}. \tag{13}$$

Since V_0^{est}, i.e. head node voltage is known, the voltage of other nodes of a radial grid can be found using (13).

Step 6: *Per-phase voltage difference* : Using (13), the difference in per-phase voltage can be found as,

$$\Delta V_i = |V_i^{\text{est}}| - |V_i^{\text{per}}| \quad \forall i \in \mathcal{V}. \tag{14}$$

Step 7: *Updating voltage bounds*: the voltage bounds are updated for $\mathbf{P}_{\text{CIA}}^{\phi,+}$ to reflect the cumulative path voltage difference that arises due to per-phase optimization neglecting mutual impedances. The update is as follows:

$$\overline{V} \leftarrow \overline{V} + \Delta V_i$$
$$\underline{V} \leftarrow \underline{V} - \Delta V_i. \tag{15}$$

Step 8: *Iterate*: Go to **Step** 1.

Next section, numerical results are presented to validate the proposed methodology.

VI. NUMERICAL RESULTS

In this section, simulation results on IEEE 37-node test system are presented together with a realistic 534-node radial distribution system from Vermont. IEEE 37-node test system is a three-phase, unbalanced medium voltage (4.8 kV) network with a total load of 2.45 MW. The realistic feeder used in this paper is a 7.2 kV radial network including 534 nodes, 533 lines, and 160 loads with a total load of 2.47 MW. The MATLAB code provided by [19] is used for three-phase simulations. Using the proposed approach enables an increase in

the HC. Fig. 5 shows the voltage bounds upon the termination of the proposed iterative method for $\mathbf{P}_{\text{CIA}}^{\phi,+}$ problem. It is important to highlight that the outcomes obtained using the **Mod-Z** method differ from those in Table II because we used the original 37-node feeder instead of its modified version from Section IV that satisfied Assumptions 1 and 2. The mutual impedance values are set as $z_{ij}^m = (z_{ij}^{\text{bc}} + z_{ij}^{\text{ac}} + z_{ij}^{\text{ab}})/3$ in the $\mathbf{P}_{\text{CIA}}^{\phi,+}$. It can be seen that all of the three-phase voltages are within $\underline{V}, \overline{V}$.

For the IEEE 37-node system, the results of p_i^- and p_i^+ obtained from three different methods—Method 2ii, Mod-Z, and the iterative HC approach—are displayed in Fig. 6. It is worth noting that the iterative method, can lead to lower nodal hosting capacity (p_i^+ and p_i^-) at some of the nodes. However, $\underline{\text{HC}}$ and $\overline{\text{HC}}$ consistently show improvements when utilizing the iterative method. This enhancement is achieved by leveraging information regarding the mutual impedance of the grid. This increase in hosting capacity does not lead to any voltage violations, therefore no line modification is required in $\mathbf{P}_{\text{CIA}}^{\phi,+}$. That is, Mod-Z is not used for iterative method.

Fig. 7 presents $|V^{3\phi}|$ for Methods 2ii and the iterative voltage bound method applied to the 534-node network for $\mathbf{P}_{\text{CIA}}^{\phi,-}$. It can be seen that using the proposed iterative method, the voltage profile becomes more unbalanced. Specifically, the VUF increases from 0.44% in Method 2ii to 1.37% in the
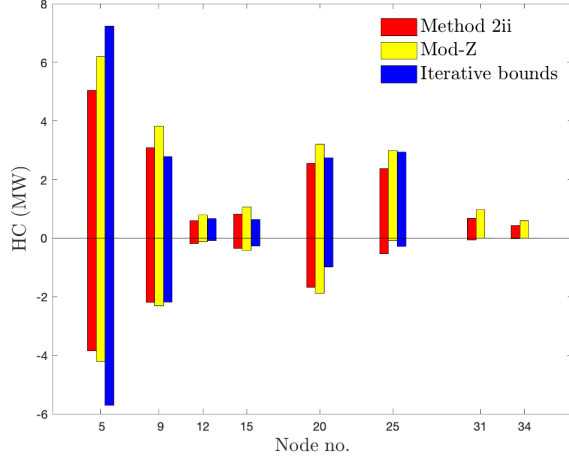
Fig. 6. Comparing the hosting capacity calculation from the iterative approach to that of Method 2ii and Mod-Z for 37-node network.
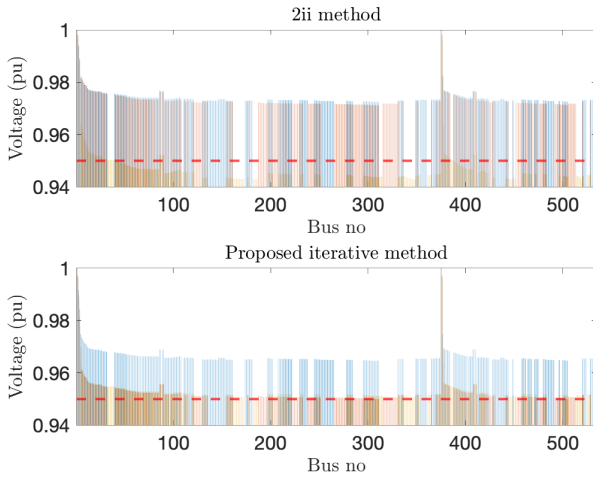

Fig. 7. Voltage profiles for 534-node feeder. The top figure illustrates the voltage profile using Method 2ii, while the bottom figure presents the voltages obtained from the proposed iterative HC method. In these figures, blue, red, and yellow correspond to phases a, b, and c, respectively.

iterative voltage bound method.

It is important to note that the optimization problem may result in very small HC values in some nodes while leading to significantly higher HC values in a few nodes within the system. This discrepancy can raise concerns regarding fairness since only certain consumers will be permitted to install DERs. We consider two sets of w_i, in the objective function and evaluate the HC for a realistic 534-node network under two scenarios: 1) Weight values (w_i) for leaf nodes are halved compared to other nodes. 2) Weight values for leaf nodes are doubled compared to other nodes. Modifying the w_i coefficients enables us to expand the locations where DERs can be installed. However, this adjustment comes at the cost of reduced $\overline{\text{HC}}$, which decreases from 78.1 MW to 27.6 MW, and reduced $\underline{\text{HC}}$, which decreases from 44.9 MW to 13.1 MW.

Future research efforts could delve into exploring the trade-off between fairness in DER allocation and its impact on the overall HC of the grid.

VII. CONCLUSION

This paper has introduced a comprehensive approach to obtaining the DER HC in a three-phase distribution feeder. Leveraging CIA of the AC power flow, our methodology establishes bounds on positive and negative DER injections at each node. A rigorous analysis is developed to ascertain the conditions under which this per-phase approach can guarantee compliance with three-phase constraints. The approach is capable of improving HC. Furthermore, we have presented an iterative approach to enhance HC by adjusting per-phase voltage bounds. A simulation-based analysis using both the IEEE 37-node test feeder and a real 534-node unbalanced radial distribution feeder is performed and results demonstrate that the proposed iterative method increases the feeder HC. Potential future research encompasses the extension of the proposed method to analyze comprehensive 3-phase networks, as well as comparing its conservativeness to the method presented in this paper. Additionally, extending the HC analysis methods to meshed distribution and sub-transmission networks will be explored in future work.

APPENDIX

A. Derivation of current proxy bounds l^- and l^+

The goal of this appendix is to clarify the structure of the affine $f_{\text{aff}}(.)$ and quadratic $f_{\text{quad}}(.)$ functions that underpin bounds l^-, l^+ used in (3). To derive the lower and upper bounds of l, we consider the second-order Taylor-series approximation of (2) about an appropriate nominal operating point, $x^0_{ij} := \text{col}\{P^0_{ij}, Q^0_{ij}, v^0_j\} \in \mathbb{R}^3$. This yields an approximation that is accurate across a range of operating conditions [10]:

$$l_{ij}(P_{ij}, Q_{ij}, V_i) \approx l^0_{ij}(x^0_{ij}) + J^\top_{ij}\delta_{ij} + \frac{1}{2}\delta^\top_{ij}H_{e,ij}\delta_{ij}, \quad (16)$$

where $\delta_{ij} := [P_{ij} - P^0_{ij}, Q_{ij} - Q^0_{ij}, v_j - v^0_j]$, the Jacobian, J_{ij}, and Hessian, $H_{e,ij}$, are defined as

$$J_{ij} := \begin{bmatrix} \dfrac{2P^0_{ij}}{v^0_i} & \dfrac{2Q^0_{ij}}{v^0_i} & -\dfrac{(P^0_{ij})^2 + (Q^0_{ij})^2}{(v^0_i)^2} \end{bmatrix}, \quad (17)$$

$$H_{e,ij} := \begin{bmatrix} \dfrac{2}{v^0_i} & 0 & \dfrac{-2P^0_{ij}}{(v^0_i)^2} \\ 0 & \dfrac{2}{v^0_i} & \dfrac{-2Q^0_{ij}}{(v^0_i)^2} \\ \dfrac{-2P^0_{ij}}{(v^0_i)^2} & \dfrac{-2Q^0_{ij}}{(v^0_i)^2} & 2\dfrac{(P^0_{ij})^2 + (Q^0_{ij})^2}{(v^0_i)^3} \end{bmatrix}. \quad (18)$$

From (16), the square of current magnitude is always positive, so:

$$l_{ij} = |l_{ij}| \approx \left| l^0_{ij} + J^\top_{ij}\delta_{ij} + \frac{1}{2}\delta^\top_{ij}H_{e,ij}\delta_{ij} \right|. \quad (19)$$

Applying the triangle inequality and the fact that Hessian in (18) is positive semi-definite (PSD) [9], we have

$$l_{ij} \leq l_{ij}^0 + \left| J_{ij}^\top \delta_{ij} \right| + \frac{1}{2} \delta_{ij}^\top H_{e,ij} \delta_{ij}. \qquad (20)$$

Applying the properties of the maximum operator, we get quadratic function:

$$l_{ij} \leq l_{ij}^0 + \max \left\{ 2 \left| J_{ij}^\top \delta_{ij} \right|, \delta_{ij}^\top H_{e,ij} \delta_{ij} \right\}. \qquad (21)$$

Note that the RHS of (21) is quadratic in terms of the three physical variables (P_{ij}, Q_{ij}, V_i) that embody δ_{ij}. To characterize the upper bound in terms of the proxy variables requires considering worst-case combinations of upper ($^+$) and lower ($^-$) proxy variables, i.e., over all eight combinations: $\delta_{ij}^+ := \delta_{ij}(P_{ij}^+, Q_{ij}^+, V_i^+)$, $\delta_{ij}(P_{ij}^+, Q_{ij}^+, V_i^-)$, ..., $\delta_{ij}(P_{ij}^-, Q_{ij}^-, V_i^+)$, and $\delta_{ij}^- := \delta_{ij}(P_{ij}^-, Q_{ij}^-, V_i^-)$. Thus, we get:

$$f_{\mathrm{quad}}(.) := l_{ij}^0 + \max \left\{ 2 \left| J_{ij,+}^\top \delta_{ij}^+ + J_{ij,-}^\top \delta_{ij}^- \right|, \psi_{ij} \right\}, \quad (22)$$

where $J_{ij,+}$ and $J_{ij,-}$ are composed of the positive and negative entries of J_{ij}, respectively, and $J_{ij} = J_{ij,+} + J_{ij,-}$. Further, $\psi_{ij} := \max\{\delta_{ij}^{+/-\top} H_{e,ij} \delta_{ij}^{+/-}\}$ is the largest product among the eight proxy pairs. Clearly, relaxing $f_{\mathrm{quad}}(.)$ provides a convex upper bound on l_{ij} as utilized in (3).

For the lower bound, consider (16) and drop the term with PSD $H_{e,ij}$, which gives

$$l_{ij} \geq l_{ij}^0 + J_{ij}^\top \delta_{ij} := \underline{l}_{ij}. \qquad (23)$$

Thus, in terms of proxy variables, we get

$$f_{\mathrm{aff}}(.) := l_{ij}^0 + J_{ij,+}^\top \delta_{ij}^- + J_{ij,-}^\top \delta_{ij}^+. \qquad (24)$$

This completes the derivations. For full details on these bounds and the CIA-based methods and results (for balanced feeders), please see [9], [10].

B. Proof of Theorem 1

From Assumption 2, the impedance matrix has identical mutual impedances z_{ij}^m, which together with (6), means that $\Delta V_{ij}^{3\phi}$ can be expressed as,

$$\Delta V_{ij}^{3\phi} = \begin{bmatrix} z_{ij}^a I_{ij}^a + z_{ij}^m (I_{ij}^b + I_{ij}^c) \\ z_{ij}^b I_{ij}^b + z_{ij}^m (I_{ij}^a + I_{ij}^c) \\ z_{ij}^c I_{ij}^c + z_{ij}^m (I_{ij}^a + I_{ij}^b) \end{bmatrix}. \qquad (25)$$

Now, under Assumption 1, $I_{ij}^a + I_{ij}^b + I_{ij}^c = 0$, which decouples the phases as

$$\Delta V_{ij}^{3\phi} = \begin{bmatrix} z_{ij}^a - z_{ij}^m & 0 & 0 \\ 0 & z_{ij}^b - z_{ij}^m & 0 \\ 0 & 0 & z_{ij}^c - z_{ij}^m \end{bmatrix} I_{ij}^{3\phi}. \qquad (26)$$

The diagonal structure clearly extends per-phase analyses to the corresponding full 3-phase (unbalanced) feeder. Thus, HC analysis via $\mathbf{P}_{\mathrm{CIA}}^{\phi,+}$ meets 3-phase voltage requirements. This concludes the proof.

REFERENCES

[1] K. Schmitt, R. Bhatta, M. Chamana, M. Murshed, I. Osman, S. Bayne, and L. Canha, "A review on active customers participation in smart grids," *Journal of Modern Power Systems and Clean Energy*, vol. 11, no. 1, pp. 3–16, 2023.

[2] M. Almassalkhi, S. Brahma, N. Nazir, H. Ossareh, P. Racherla, S. Kundu, S. P. Nandanoori, T. Ramachandran, A. Singhal, D. Gayme, C. Ji, E. Mallada, Y. Shen, P. You, and D. Anand, "Hierarchical, grid-aware, and economically optimal coordination of distributed energy resources in realistic distribution systems," *Energies*, vol. 13, no. 23, 2020. [Online]. Available: https://www.mdpi.com/1996-1073/13/23/6399

[3] AusNet Services. (2017) . export limits for embedded generators up to 200 kva connected at low voltage. [Online]. Available: https://www.ausnetservices.com.au/

[4] M. Z. Liu, L. F. Ochoa, P. K. C. Wong, and J. Theunissen, "Using opf-based operating envelopes to facilitate residential der services," *IEEE Transactions on Smart Grid*, vol. 13, no. 6, pp. 4494–4504, 2022.

[5] X. Chen, E. Dall'Anese, C. Zhao, and N. Li, "Aggregate power flexibility in unbalanced distribution systems," *IEEE Transactions on Smart Grid*, vol. 11, no. 1, pp. 258–269, 2020.

[6] E. Dall'Anese, S. S. Guggilam, A. Simonetto, Y. C. Chen, and S. V. Dhople, "Optimal regulation of virtual power plants," *IEEE Transactions on Power Systems*, vol. 33, no. 2, pp. 1868–1881, 2018.

[7] Z. Yuan and M. Reza Hesamzadeh, "A distributed economic dispatch mechanism to implement distribution locational marginal pricing," in *2018 Power Systems Computation Conference (PSCC)*, 2018, pp. 1–7.

[8] S. Ross and J. Mathieu, "Strategies for network-safe load control with a third-party aggregator and a distribution operator," *IEEE Transactions on Power Systems*, vol. 36, no. 4, pp. 3329–3339, 2021.

[9] N. Nazir and M. Almassalkhi, "Voltage positioning using co-optimization of controllable grid assets in radial networks," *IEEE Transactions on Power Systems*, vol. 36, no. 4, pp. 2761–2770, 2021.

[10] N. Nzir and M. Almassalkhi, "Grid-aware aggregation and realtime disaggregation of distributed energy resources in radial networks," *IEEE Transactions on Power Systems*, vol. 37, no. 3, pp. 1706–1717, 2022.

[11] D. Lee, K. Turitsyn, D. K. Molzahn, and L. A. Roald, "Feasible path identification in optimal power flow with sequential convex restriction," *IEEE Transactions on Power Systems*, vol. 35, no. 5, pp. 3648–3659, 2020.

[12] D. Lee, K. Turitsyn, D. K. Molzahn, and L. Roald, "Robust AC optimal power flow with robust convex restriction," *IEEE Transactions on Power Systems*, vol. 36, no. 6, pp. 4953–4966, 2021.

[13] V. Bassi, D. Jaglal, L. Ochoa, T. Alpcan, and C. Leckie, "Deliverables 1-2-3a model-free voltage calculations and operating envelopes," University of Melbourne, Technical Report, 7 2022.

[14] K. Petrou, A. T. Procopiou, L. Gutierrez-Lagos, M. Z. Liu, L. F. Ochoa, T. Langstaff, and J. M. Theunissen, "Ensuring distribution network integrity using dynamic operating limits for prosumers," *IEEE Transactions on Smart Grid*, vol. 12, no. 5, pp. 3877–3888, 2021.

[15] V. Rigoni, D. Flynn, and A. Keane, "Coordinating demand response aggregation with lv network operational constraints," *IEEE Transactions on Power Systems*, vol. 36, no. 2, pp. 979–990, 2021.

[16] M. Baran and F. Wu, "Optimal capacitor placement on radial distribution systems," *IEEE Transactions on Power Delivery*, vol. 4, no. 1, pp. 725–734, Jan. 1989. [Online]. Available: http://ieeexplore.ieee.org/document/19265/

[17] R. Heidari, M. M. Seron, and J. H. Braslavsky, "Non-local approximation of power flow equations with guaranteed error bounds," in *2017 Australian and New Zealand Control Conference (ANZCC)*, 2017, pp. 83–88.

[18] K. P. Schneider, B. A. Mather, B. C. Pal, C.-W. Ten, G. J. Shirek, H. Zhu, J. C. Fuller, J. L. R. Pereira, L. F. Ochoa, L. R. de Araujo, R. C. Dugan, S. Matthias, S. Paudyal, T. E. McDermott, and W. Kersting, "Analytic Considerations and Design Basis for the IEEE Distribution Test Feeders," *IEEE Transactions on Power Systems*, vol. 33, no. 3, pp. 3181–3188, 2018.

[19] A. Garces. (2023) Linear load flow in power distribution systems: Unbalanced case. Online. MATLAB Central File Exchange. Retrieved September 23, 2023. [Online]. Available: https://www.mathworks.com/matlabcentral/fileexchange/56074-linear-load-flow-in-power-distribution-systems-unbalanced-case